Cuproptosis-related lncRNAs are correlated with metabolism and immune microenvironment and predict prognosis in pancreatic cancer patients

Yanling Wang
Department of Oncology, Renji Hospital Affiliated to Shanghai Jiao Tong University School of Medicine, Shanghai Cancer Institute, Shanghai

Weiyu Ge
Department of Oncology, Renji Hospital Affiliated to Shanghai Jiao Tong University School of Medicine, Shanghai Cancer Institute, Shanghai

Shengbai Xue
Department of Oncology, Renji Hospital Affiliated to Shanghai Jiao Tong University School of Medicine, Shanghai Cancer Institute, Shanghai

Jiujie Cui
Department of Oncology, Renji Hospital Affiliated to Shanghai Jiao Tong University School of Medicine, Shanghai Cancer Institute, Shanghai

Xiaofei Zhang
Department of Oncology, Renji Hospital Affiliated to Shanghai Jiao Tong University School of Medicine, Shanghai Cancer Institute, Shanghai

Daiyuan Shentu
Department of Oncology, Renji Hospital Affiliated to Shanghai Jiao Tong University School of Medicine, Shanghai Cancer Institute, Shanghai

Liwei Wang (liweiwang@shsmu.edu.cn)
Department of Oncology, Renji Hospital Affiliated to Shanghai Jiao Tong University School of Medicine, Shanghai Cancer Institute, Shanghai

---

Research Article

Keywords: pancreatic cancer, cuproptosis, lncRNA, prognostic model, metabolism, immune microenvironment

Posted Date: May 16th, 2022

DOI: https://doi.org/10.21203/rs.3.rs-1645540/v1

Abstract

Background: Cuproptosis is a novel cell death pathway, and the regulatory mechanism in pancreatic cancer (PC) remains to be explored. We determined whether cuproptosis-related lncRNAs (CRLs) could predict prognosis in pancreatic cancer.

Methods and results: First, we identified 30 prognostic cuproptosis-related lncRNAs by Pearson correlation and univariate Cox regression analyses. Next, we constructed the cuproptosis-related lncRNAs prognostic model based on seven CRLs screened by the least absolute shrinkage and selection operator (LASSO) Cox analysis. Following this, we calculated the risk score for pancreatic cancer patients according to the formula and divided patients into high and low-risk groups. In our prognostic model, PC patients with higher risk scores had poorer outcomes. Based on several prognostic features, a predictive nomogram was established in PC. Furthermore, we investigated the tumor immune landscape using CIBERSORT and ESTIMATE. The tumor microenvironment in the high-risk group was more immunosuppressive than that in the low-risk group, with lower infiltration of CD8+ T cells and higher M2 macrophages. Finally, we performed the functional enrichment analysis of 181 differentially expressed genes (DEGs) between risk groups. Our results revealed that endocrine and metabolic pathways were potential regulatory pathways between risk groups.

Conclusion: Cuproptosis-related lncRNAs can be applied to predict pancreatic cancer prognosis, which is closely correlated with the tumor metabolism and immune microenvironment.

Introduction

Pancreatic cancer (PC) is a highly malignant disease with a 5-year survival rate of less than 10% [1]. Surgical resection is curative, but approximately 80% of patients are already unresectable at diagnosis [2]. Patients with advanced PC benefit a little from chemotherapy and quickly develop resistance to it. Furthermore, a majority of clinical trials in PC failed to achieve clinically meaningful survival benefit. With the development of precision medicine technologies, we could find certain groups of patients benefit from therapies. Consequently, investigating more druggable targets for PC patients is a continuing concern.

Copper ionophore-induced cell death termed cuproptosis reveals a new cell death pathway that differs from apoptosis, ferroptosis, pyroptosis, and necroptosis [3]. Peter Tsvetkov et al. first reported that copper ionophore-induced cell death was closely correlated with mitochondrial respiration and protein lipoylation. FDX1 is a key regulator of cuproptosis, and the deletion of FDX1 protects cells from cuproposis. Elesclomol, a potent copper ionophore, displayed a tumor-killing effect by cuproptosis. Although it had failed in phase 3 clinical trial, elesclomol was verified antitumor activity in melanoma patients with low plasma lactate dehydrogenase levels [4]. This gives us insights that we can identify cuproptosis-sensitive tumor patients to treat with cooper ionophores. With more in-depth studies of the mechanism of cuproptosis, copper toxicity could be utilized as an antitumor mechanism in specific groups of patients.

Long non-coding RNAs (lncRNAs) play a role in a series of signaling pathways in tumorigenesis, growth, and metastasis [5]. In pancreatic cancer, lncRNA RGMB-AS1 and CYTOR promote cancer cell proliferation and migration [6, 7]. LncRNAs can promote gemcitabine resistance in pancreatic cancer, such as PVT1 and HIF1A-AS1 [8, 9]. PVT1 was reported to activate Wnt/β-catenin and autophagy pathway. However, HIF1A-AS1 enhances glycolysis via the AKT/YB1/HIF1α Pathway. Moreover, some lncRNAs were proved to regulate cancer cell apoptosis [10], ferroptosis [11], and pyroptosis [12].

Our study aimed to construct a cuproptosis-related lncRNAs (CRLs) prognostic model in pancreatic cancer using The Cancer Genome Atlas (TCGA) datasets. Figure 1 presents the workflow of our study. We identified seven prognostic CRLs and constructed and validated our prognostic model using bioinformatics. Additionally, we analyzed the tumor immune microenvironment in risk groups. At last, we performed the functional enrichment analysis to figure out potential signaling pathways in risk groups.

Results

Identification of prognostic CRLs

We downloaded the Pancreatic cancer datasets from TCGA database, which included 177 tumor samples and 4 normal samples (samples without expression matrix or clinical information were excluded). Table 1 exhibited the clinical characteristics of pancreatic cancer patients. According to the GENCODE database, we identified 14084 lncRNAs from TCGA pancreatic cancer dataset. According to the previous study, there are ten cuproptosis regulators (FDX1, LIAS, LIPT1, DLD, DLAT, GLS, PDHA1, PDHB, MTF1, CDKN2A) [3]. After obtaining the expression matrix of 10 cuproptosis regulators, Pearson correlation analysis was performed (|Pearson R| > 0.4, $p < 0.001$) and we obtained 40 CRLs. Finally, to identify prognostic CRLs, we used the univariate Cox regression analysis ($p < 0.05$). The hazard ratio and expression of 30 prognostic CRLs were shown in Fig. 2A-C.

Table 1
Clinical characteristics of PC patients in TCGA dataset

Clinical characteristics	Count
Age	
<=65	93
> 65	84
Gender	
Female	80
Male	97
Grade	
G1	31
G2	94
G3	48
G4	2
Gx	2
T stage	
T1	7
T2	24
T3	141
T4	3
Tx	2
M stage	
M0	79
M1	4
Mx	94
N stage	
N0	50
N1	123
Nx	4

Clinical characteristics	Count
Tumor site	
Head of pancreas	138
Others	39

Construction and validation of the CRLs prognostic model

To construct the cuproptosis-related lncRNAs prognostic model in PC, we performed the least absolute shrinkage and selection operator (LASSO) Cox regression. PC patients from the dataset were randomly assigned to the training and test cohort. As a result, 7 of 30 prognostic CRLs ($p < 0.01$) were filtered to build the prognostic model (Fig. 3A-B). The following formula was used to compute each patient's risk score: risk score = (-0.327099393974077 * PAN3-AS1 expression) – (0.29606012121351 * LINC02593 expression) – (1.37664328433923 * AL117335.1 expression) – (0.498179055188389 * LINC01091 expression) – (0.0197617573760847 * AC092171.3 expression) – (0.237742487425625 * AC087501.4 expression) – (1.04195463033265 * SUGT1P4-STRA6LP expression). Patients were classified as high or low risk based on their median risk score (Fig. 3C-F). PAN3-AS1, LINC02593, AL117335.1, LINC01091, AC092171.3, AC087501.4, and SUGT1P4-STRA6LP were downregulated in the high-risk group. (Fig. 3G).

It's apparent from the survival analysis that PC patients with a low-risk score enjoyed a better prognosis in the training cohort ($p < 0.001$, Fig. 4A). We conducted the time-dependent receiver operating characteristic (ROC) analysis to assess the predictive power of the risk model. The area under curve (AUC) of the ROC greater than 0.5 was considered to have good predictive capacity. In the training group, AUC values at years 1, 2, and 3 were all greater than 0.7 (0.719, 0.786, and 0.803, respectively, Fig. 4B). Compared with other clinical characteristics, our risk model also performed well in predictive capacity (Fig. 4C). Then we validated our risk model in the test cohort. It’s also verified that there was a significant difference in overall survival (OS) between the two risk groups ($p = 0.025$, Fig. 4D). In the test cohort, our risk model was shown to have the precise predictive capability, and the AUC values at years 1, 2, and 3 were 0.658, 0.690, and 0.666, respectively (Fig. 4E-F).

The training and test cohorts were then subjected to univariate and multivariate Cox regression analysis (Fig. 4G-J). Tumor tissue grade and risk score were negatively correlated with pancreatic cancer prognosis in the training cohort ($p = 0.001$ and $p < 0.001$ in multivariate analysis, respectively). The risk score was likewise validated as an independent prognostic factor, in the test cohort ($p = 0.01$).

Independence analyses of the prognostic model

Following that, we looked into the relationship between risk scores and clinicopathological variables (Fig. 5A-F). T stage was found to be significantly related to risk score ($p = 0.0021$), with individuals with T3-4 stage tumors having higher risk scores. The risk score, on the other hand, was adversely linked with

the tumor immune score ($p = 0.0044$). Other clinicopathological factors such as age, gender, tumor site and tissue grade didn't correlate with the risk score.

Figure 5G depicts a heatmap showing the relationship between the expression levels of seven prognostic CRLs and clinicopathological characteristics of individuals. The high-risk group had significantly higher CIBERSORT immune scores than the low-risk group ($p < 0.05$). Furthermore, we confirmed that our prognostic model can be used in different subgroups of pancreatic cancer patients (Fig. 5H-O). The prognostic model performed well in the female/male subgroup, T1-2/T3-4 stage subgroup, N0/N1-3 stage subgroup, and different tumor site subgroups. Patients in the low-risk category still enjoyed a superior outcome in these subgroups.

Construction of the OS nomogram

We created a predictive nomogram based on four prognostic factors, including risk score, age, tumor tissue grade, and tumor site (head of pancreas and others) to directly predict the overall survival of PC patients (Fig. 6A). It's easy to know the probabilities of 1-, 2-, and 3-year OS by calculating total points. Finally, the calibration curve revealed that the predicted and actual probabilities were in good agreement (Fig. 6B).

Immunity and tumor purity analyses between risk groups

Next, the immune status of the risk groups was determined through CIBERSORT immune analysis. We discovered a negative relationship between risk scores and the infiltration of CD8 + T cells ($p = 0.0041$, Fig. 7A), regulatory T cells ($p = 0.016$, Fig. 7B), naïve B cells ($p = 0.00036$, Fig. 7C), and plasma cells ($p = 0.048$, Fig. 7D). Meanwhile, the risk score was positively correlated with abundance of M0 macrophages ($p = 0.0066$, Fig. 7E) and M2 macrophages ($p = 0.0073$, Fig. 7F). In terms of naïve B cells, plasma cells, memory B cells, CD8 + T cells, and M0 and M1 macrophages fraction, there were substantial disparities between the two risk groups (Fig. 7G). The high-risk group had higher tumor purity than the low-risk group, according to our findings ($p < 0.05$, Fig. 7H). The immune scores and ESTIMATE scores were higher in the low-risk group than in the high-risk group ($p < 0.01$ and $p < 0.05$, respectively, Fig. 7I).

DEGs and enrichment analyses

To find potential regulatory pathways, we identified DEGs between risk groups. As a consequence, the high-risk group had 31 upregulated genes and 150 downregulated genes when compared to the low-risk group (log2 | FC | > 1.5, $p < 0.01$, Fig. 8A). DEGs were significantly enriched in the endocrine and metabolic-related signaling pathways, including the secretion and transport of insulin and other peptide hormones, according to Gene Ontology (GO) enrichment analysis (Fig. 8B-D). Kyoto Encyclopedia of Genes and Genomes (KEGG) enrichment analysis also revealed DEGs were enriched in metabolic signaling pathways, including calcium signaling pathway, cytokine – cytokine receptor interaction, cAMP signaling pathway, and so on (Fig. 8E-F).

Discussion

Pancreatic cancer is notorious cancer with high mortality rates. Most PC patients have metastases at diagnosis, thus chemotherapy is the most common treatment option. Nab-paclitaxel–gemcitabine (AG) and fluorouracil, leucovorin, irinotecan, and oxaliplatin (FOLFIRINOX) are advised for patients with good performance status, but the median overall survival remained frustrating at 8.7 and 11.1 months, respectively [13, 14]. KRAS, CDKN2A, TP53, and SMAD4 are the most frequently mutated genes in pancreatic cancer, however, none of them are currently druggable except KRAS G12C [15, 16]. A list of antiangiogenic drugs, such as the vascular endothelial growth factor (VEGF) inhibitors aflibercept and bevacizumab, have failed in clinical trials due to a lack of blood vessels in the stroma around cancer cells [17, 18]. As for immunotherapy, for pancreatic patients with a positive dMMR/MSI-H, humanized monoclonal anti-PD1 antibody pembrolizumab has been suggested as a second-line therapy [19].

A series of copper complexes were reported to induce apoptosis in PC, such as Cu (II) complex of ketoprofen-salicylhydrazone (FPA-306) and tolfenamic acid–Cu (II) complex [20, 21]. In addition, copper complex $[Cu^{II}_2Cu^{I}(L)_2(Br)_3]$ kills pancreatic cancer via nonapoptotic cell death pathways, including ferroptosis [22]. Recently, elesclomol was shown to induce cell death via cuproptosis after inhibiting ferroptosis, necroptosis, and oxidative stress [3]. Taken together, we suspect that some copper complexes might induce pancreatic cancer cell death via cuproptosis. Cuproptosis is a promising way to induce tumor cell death, and this research aimed to investigate cuproptosis -related lncRNAs and prognostic biomarkers in PC.

Our study identified 30 prognostic CRLs with univariate Cox regression analysis, and most of them were downregulated in tumor tissues. Then, seven prognostic CRLs filtered by LASSO Cox analysis were used to build a prognostic model. In our prognostic model, high-risk PC patients had a poor prognosis and lower expressions of these prognostic CRLs, which was validated in our test group. The AUC values of the model were greater than 0.7 at 1, 2, and 3 years. Compared with other clinical risk factors, our model showed better prediction performance. The risk score was closely related to the prognosis of PC patients by univariate and multivariate Cox regression analyses. Next, we verified our prognostic model can be used in PC groups with specific clinicopathological characteristics, such as female/male groups, T1-2/T3-4 stage groups, N0/N1-3 stage groups, and different tumor site groups. In addition, we constructed a nomogram that combined clinical prognostic characteristics to predict 1-, 2- and 3-year survival.

Then, we investigated the tumor microenvironment in our risk model by CIBERSORT and ESTIMATE. The risk score was found to have a negative correlation with CD8 + T cells, and a positive correlation with M0 and M2 macrophages. Patients in the low-risk group had a higher fraction of CD8 + T cells, naïve B cells, and plasma cells and a higher immune score than that in the high-risk group. Consistent with previous research, the microenvironment of pancreatic cancer is immunosuppressive, enriched with myeloid-derived suppressor cells (MDSC), tumor-associated macrophages, and Tregs [23]. M1 macrophages exhibit pro-inflammation, while M2 macrophages suppress immunity and promote tumor growth and

angiogenesis [24]. Tregs act as anti-tumor immunity in PC, suppressing dendritic cells and CD8 + T cells[25]. Indeed, low CD8 + T cells and high macrophages and Tregs in pancreatic cancer were correlated with poor survival [26, 27]. Patients with high-risk scores were more likely to have cold tumors which deficient in T cells but rich in tumor-associated macrophages (TAMs). Cold tumors are more insensitive to immune checkpoint inhibitors due to low immunogenicity than hot tumors [28, 29]. In our study, there was no statistical difference in the stroma score between the risk groups, but the tumor purity was higher in the high-risk group than in the low-risk group.

Next, we performed to further explore possible regulatory pathways. DEGs between the two risk groups were enriched in endocrine and metabolic-related pathways. DEGs enriched in insulin and other peptide hormone signaling pathways in the GO analysis. Diabetes is verified as a risk factor for pancreatic cancer in previous studies [30]. Insulin/insulin-like growth factor 1(IGF-1) receptors and G protein-coupled receptors (GPCR) signaling systems regulate the proliferation of pancreatic cancer and chemoresistance [31, 32]. Metformin can inhibit the insulin-GPCR crosstalk and decrease the risk of pancreatic cancer [31]. DEGs enriched in several metabolic signaling pathways in KEGG enrichment analysis. Calcium signaling which is correlated with gene transcription and cell proliferation regulates early pancreatic carcinogenesis [33–35]. Cancer metabolism alters the immune microenvironment to immunosuppressive status to promote tumor progression. Increased glycolysis and lactate production in tumor cells leads to immunosuppression of the tumor microenvironment, manifested by increased M2 macrophage polarization, increased Tregs, and decreased CD8 + T cells [36–38]. Meanwhile, TAMs secreted CCL18 promoting the Warburg effect in pancreatic cancer [39]. Pancreatic cancer cells are in a relatively hypoxic environment due to dense stroma and low perfusion. Kras G12D mutation is critical for the regulation of glucose metabolism in pancreatic cancer [40]. However, cuproptosis relies on mitochondrial metabolism and the tricarboxylic acid cycle. The intracellular copper buildup causes mitochondrial lipoylated proteins to aggregate and Fe-S cluster proteins to destabilize, resulting in cell death. Glycolysis-dominated tumor cells are less susceptible to cuproptosis [3]. Inhibition of tumor cell glycolysis may increase sensitivity to copper ionophore therapy.

Above all, we recognized seven prognostic cuproptosis-related lncRNAs and provided a new prognostic model for PC patients that predicts overall survival. We verified that cuproptosis was related to tumor metabolism and the immune microenvironment. Cuproptosis is a newly discovered way of cell death with many unknown mechanisms waiting to be explored. We can induce cuproptosis using copper ionophores in cuproptosis-sensitive tumors. Even we can alter TME through cuproptosis, making it easier for anti-tumor drugs to enter tumor cells.

Our study has some limitations. First, we only used TCGA datasets to construct and validate our prognostic model. We are carrying out experiments to explore the role of cuproptosis regulators in PC *in vivo* and *vitro*. Second, in TCGA dataset, it lacked PC patients with metastasis. We are collecting clinical data in our institution to validate our prognostic signature. In addition, more regulators in cuproptosis need to be explored to further investigate their roles in pancreatic cancer.

Conclusion

In conclusion, this study identified prognostic CRLs and construct a prognostic model of pancreatic cancer. Furthermore, we elucidated that the CRLs influenced the prognosis of PC via regulating the metabolism and immune microenvironment. Our finding might provide some clews of pancreatic cancer therapy and prognostic prediction.

Materials And Methods

Datasets

The RNA sequencing data of PC and clinical characteristics were obtained from the TCGA database (https://portal.gdc.cancer.gov), including 177 PC patients and 4 normal pancreatic tissues (samples without expression matrix or clinical information were excluded). Then the expression of lncRNAs was extracted according to the human gene annotations in GENCODE (https://www.gencodegenes.org/). Cuproptosis regulators were obtained from the previous study (FDX1, LIAS, LIPT1, DLD, DLAT, GLS, PDHA1, PDHB, MTF1, CDKN2A) [3].

Bioinformatic analysis

Our bioinformatic analysis was based on the “R” (version 4.1.3) software. We identified cuproptosis-related lncRNA by the “limma” package in the “R” (|Pearson R| > 0.4, $p < 0.001$). Then we obtained prognostic CRLs through the univariate Cox regression analysis ($p < 0.05$) with the “survival” package. We performed Lasso cox regression analysis with the “glmnet” package to construct the prognostic model. The risk score was calculated according to the formula:

Risk score = $\sum Coef * EXP$.

In this formula, Coef is the coefficient and EXP is the expression level of each prognostic cuproptosis-related lncRNAs. PC patients were grouped based on the value of risk scores. Kaplan-Meier survival curves were drawn via the “survminer” package, and ROC curves were drawn by the “timeROC” package.

We calculated the fraction of 22 tumor-infiltrating immune cells using CIBERSORT. ESTIMATE scores in tumor tissues were calculated using the “estimate” package. DEGs between risk categories were filtered using the “limma” package (|log2FoldChange| > 1.5, $p < 0.01$). The DEGs were performed GO and KEGG enrichment analyses via “clusterProfiler” package. A nomogram was constructed using the “rms” package.

Statistical analysis

Cuproptosis-related lncRNAs were identified by Pearson correlation test. To compare overall survival between subgroups, Kaplan-Meier (KM) analysis was used. The difference in risk scores between subgroups was compared using the student’s t-test, and categorical variables of groups were analyzed by

chi-square test. The correlation among subtypes was calculated using the Pearson correlation test. We explored the independent prognostic value of the risk scores and other clinical features using univariate and multivariate Cox regression analyses. Statistical analysis was conducted by the “R” software. In our study, a *p*-value of less than 0.05 was considered statistically significant.

Abbreviations

PC: pancreatic cancer

lncRNA: long non-coding RNA

CRL: cuproptosis-related lncRNA

TCGA: The Cancer Genome Atlas

DEG: differentially expressed gene

LASSO: least absolute shrinkage and selection operator

ROC: receiver operating characteristic

AUC: area under curve

OS: overall survival

GO: Gene Ontology

KEGG: Kyoto Encyclopedia of Genes and Genomes

AG: nab-paclitaxel–gemcitabine

FOLFIRINOX: fluorouracil, leucovorin, irinotecan, and oxaliplatin

VEGF: vascular endothelial growth factor

MDSC: myeloid-derived suppressor cell

TAM: tumor-associated macrophage

IGF-1: insulin-like growth factor 1

GPCR: G protein-coupled receptor

Declarations

Ethics approval and consent to participate

Not applicable.

Consent for publication:

Not applicable.

Availability of data and materials:

TCGA datasets are available through the URL: https://portal.gdc.cancer.gov

Competing interests:

The authors declare that they have no known competing interest that could influence reported in this paper.

Funding:

This study was funded by the Innovation Group Project of Shanghai Municipal Health Commission (2019CXJQ03), National Natural Science Foundation of China (81874048, 82171824), Shanghai Municipal Commission of Health and Family Planning (2018ZHYL0223), Fostering Fund of Renji Hospital Affiliated to Shanghai Jiao Tong University School of Medicine (PYIV-17-001), Clinical Research Plan of SHDC (No. SHDC2020CR1035B), Shanghai Key Clinical Speciality (Oncology), Shanghai Leading Talents Project, and Innovative Research Team of High-level Local Universities in Shanghai.

Authors' contributions:

Yanling Wang analyzed data and write the original manuscript. Weiyu Ge and Shengbai Xue validated the analyses. Jiujie Cui, Xiaofei Zhang and Daiyuan Shentu reviewed and edited the manuscript. Liwei Wang designed and supervised the study.

Acknowledgements:

Not applicable.

Authors' information:

(First author) Yanling Wang: M.D., department of Oncology, Renji Hospital Affiliated to Shanghai Jiao Tong University School of Medicine, Shanghai Cancer Institute, Shanghai, China; State Key Laboratory of Oncogenes and Related Genes, Shanghai Cancer Institute, Department of Oncology, Renji Hospital, School of Medicine, Shanghai Jiao Tong University, Shanghai, China.

(Corresponding author) Liwei Wang: M.D., Ph.D., department of Oncology, Renji Hospital Affiliated to Shanghai Jiao Tong University School of Medicine, Shanghai Cancer Institute, Shanghai, China; State Key

Laboratory of Oncogenes and Related Genes, Shanghai Cancer Institute, Department of Oncology, Renji Hospital, School of Medicine, Shanghai Jiao Tong University, Shanghai, China.

References

1. SIEGEL R L, MILLER K D, FUCHS H E, et al. Cancer Statistics, 2021 [J]. CA Cancer J Clin, 2021, 71(1): 7-33.
2. KLEEFF J, KORC M, APTE M, et al. Pancreatic cancer [J]. Nat Rev Dis Primers, 2016, 2: 16022.
3. TSVETKOV P, COY S, PETROVA B, et al. Copper induces cell death by targeting lipoylated TCA cycle proteins [J]. Science, 2022, 375(6586): 1254-61.
4. O'DAY S J, EGGERMONT A M, CHIARION-SILENI V, et al. Final results of phase III SYMMETRY study: randomized, double-blind trial of elesclomol plus paclitaxel versus paclitaxel alone as treatment for chemotherapy-naive patients with advanced melanoma [J]. J Clin Oncol, 2013, 31(9): 1211-8.
5. PENG W X, KOIRALA P, MO Y Y. LncRNA-mediated regulation of cell signaling in cancer [J]. Oncogene, 2017, 36(41): 5661-7.
6. SONG W, SHI C. LncRNA RGMB-AS1 facilitates pancreatic cancer cell proliferation and migration but inhibits cell apoptosis via miR-574-3p/PIM3 axis [J]. Am J Physiol Gastrointest Liver Physiol, 2021, 321(5): G477-g88.
7. ZHU H, SHAN Y, GE K, et al. LncRNA CYTOR promotes pancreatic cancer cell proliferation and migration by sponging miR-205-5p [J]. Pancreatology, 2020, 20(6): 1139-48.
8. ZHOU C, YI C, YI Y, et al. LncRNA PVT1 promotes gemcitabine resistance of pancreatic cancer via activating Wnt/β-catenin and autophagy pathway through modulating the miR-619-5p/Pygo2 and miR-619-5p/ATG14 axes [J]. Mol Cancer, 2020, 19(1): 118.
9. XU F, HUANG M, CHEN Q, et al. LncRNA HIF1A-AS1 Promotes Gemcitabine Resistance of Pancreatic Cancer by Enhancing Glycolysis through Modulating the AKT/YB1/HIF1α Pathway [J]. Cancer Res, 2021, 81(22): 5678-91.
10. ZHANG L, LI C, SU X. Emerging impact of the long noncoding RNA MIR22HG on proliferation and apoptosis in multiple human cancers [J]. J Exp Clin Cancer Res, 2020, 39(1): 271.
11. WANG Z, CHEN X, LIU N, et al. A Nuclear Long Non-Coding RNA LINC00618 Accelerates Ferroptosis in a Manner Dependent upon Apoptosis [J]. Mol Ther, 2021, 29(1): 263-74.
12. HE D, ZHENG J, HU J, et al. Long non-coding RNAs and pyroptosis [J]. Clin Chim Acta, 2020, 504: 201-8.
13. VON HOFF D D, ERVIN T, ARENA F P, et al. Increased survival in pancreatic cancer with nab-paclitaxel plus gemcitabine [J]. N Engl J Med, 2013, 369(18): 1691-703.
14. CONROY T, DESSEIGNE F, YCHOU M, et al. FOLFIRINOX versus gemcitabine for metastatic pancreatic cancer [J]. N Engl J Med, 2011, 364(19): 1817-25.
15. KAMISAWA T, WOOD L D, ITOI T, et al. Pancreatic cancer [J]. Lancet, 2016, 388(10039): 73-85.

16. HONG D S, FAKIH M G, STRICKLER J H, et al. KRAS(G12C) Inhibition with Sotorasib in Advanced Solid Tumors [J]. N Engl J Med, 2020, 383(13): 1207-17.
17. KINDLER H L, NIEDZWIECKI D, HOLLIS D, et al. Gemcitabine plus bevacizumab compared with gemcitabine plus placebo in patients with advanced pancreatic cancer: phase III trial of the Cancer and Leukemia Group B (CALGB 80303) [J]. J Clin Oncol, 2010, 28(22): 3617-22.
18. ROUGIER P, RIESS H, MANGES R, et al. Randomised, placebo-controlled, double-blind, parallel-group phase III study evaluating aflibercept in patients receiving first-line treatment with gemcitabine for metastatic pancreatic cancer [J]. Eur J Cancer, 2013, 49(12): 2633-42.
19. SOHAL D P S, KENNEDY E B, KHORANA A, et al. Metastatic Pancreatic Cancer: ASCO Clinical Practice Guideline Update [J]. J Clin Oncol, 2018, 36(24): 2545-56.
20. AHMED F, ADSULE S, ALI A S, et al. A novel copper complex of 3-benzoyl-alpha methyl benzene acetic acid with antitumor activity mediated via cyclooxygenase pathway [J]. Int J Cancer, 2007, 120(4): 734-42.
21. HURTADO M, SANKPAL U T, KABA A, et al. Novel Survivin Inhibitor for Suppressing Pancreatic Cancer Cells Growth via Downregulating Sp1 and Sp3 Transcription Factors [J]. Cell Physiol Biochem, 2018, 51(4): 1894-907.
22. GOU Y, CHEN M, LI S, et al. Dithiocarbazate-Copper Complexes for Bioimaging and Treatment of Pancreatic Cancer [J]. J Med Chem, 2021, 64(9): 5485-99.
23. CLARK C E, HINGORANI S R, MICK R, et al. Dynamics of the immune reaction to pancreatic cancer from inception to invasion [J]. Cancer Res, 2007, 67(19): 9518-27.
24. MANTOVANI A, SOZZANI S, LOCATI M, et al. Macrophage polarization: tumor-associated macrophages as a paradigm for polarized M2 mononuclear phagocytes [J]. Trends Immunol, 2002, 23(11): 549-55.
25. JANG J E, HAJDU C H, LIOT C, et al. Crosstalk between Regulatory T Cells and Tumor-Associated Dendritic Cells Negates Anti-tumor Immunity in Pancreatic Cancer [J]. Cell Rep, 2017, 20(3): 558-71.
26. HIRAOKA N, ONOZATO K, KOSUGE T, et al. Prevalence of FOXP3+ regulatory T cells increases during the progression of pancreatic ductal adenocarcinoma and its premalignant lesions [J]. Clin Cancer Res, 2006, 12(18): 5423-34.
27. BAILEY P, CHANG D K, NONES K, et al. Genomic analyses identify molecular subtypes of pancreatic cancer [J]. Nature, 2016, 531(7592): 47-52.
28. CHEN Q, SUN T, JIANG C. Recent Advancements in Nanomedicine for 'Cold' Tumor Immunotherapy [J]. Nanomicro Lett, 2021, 13(1): 92.
29. BEAR A S, VONDERHEIDE R H, O'HARA M H. Challenges and Opportunities for Pancreatic Cancer Immunotherapy [J]. Cancer Cell, 2020, 38(6): 788-802.
30. BOSETTI C, ROSATO V, LI D, et al. Diabetes, antidiabetic medications, and pancreatic cancer risk: an analysis from the International Pancreatic Cancer Case-Control Consortium [J]. Ann Oncol, 2014, 25(10): 2065-72.

31. KISFALVI K, EIBL G, SINNETT-SMITH J, et al. Metformin disrupts crosstalk between G protein-coupled receptor and insulin receptor signaling systems and inhibits pancreatic cancer growth [J]. Cancer Res, 2009, 69(16): 6539-45.
32. IRELAND L, SANTOS A, AHMED M S, et al. Chemoresistance in Pancreatic Cancer Is Driven by Stroma-Derived Insulin-Like Growth Factors [J]. Cancer Res, 2016, 76(23): 6851-63.
33. GREGÓRIO C, SOARES-LIMA S C, ALEMAR B, et al. Calcium Signaling Alterations Caused by Epigenetic Mechanisms in Pancreatic Cancer: From Early Markers to Prognostic Impact [J]. Cancers (Basel), 2020, 12(7).
34. SCHAAL C, PADMANABHAN J, CHELLAPPAN S. The Role of nAChR and Calcium Signaling in Pancreatic Cancer Initiation and Progression [J]. Cancers (Basel), 2015, 7(3): 1447-71.
35. ZHAO Y, SCHOEPS B, YAO D, et al. mTORC1 and mTORC2 Converge on the Arp2/3 Complex to Promote Kras(G12D)-Induced Acinar-to-Ductal Metaplasia and Early Pancreatic Carcinogenesis [J]. Gastroenterology, 2021, 160(5): 1755-70.e17.
36. CERTO M, TSAI C H, PUCINO V, et al. Lactate modulation of immune responses in inflammatory versus tumour microenvironments [J]. Nat Rev Immunol, 2021, 21(3): 151-61.
37. COLEGIO O R, CHU N Q, SZABO A L, et al. Functional polarization of tumour-associated macrophages by tumour-derived lactic acid [J]. Nature, 2014, 513(7519): 559-63.
38. PORTA C, MARINO A, CONSONNI F M, et al. Metabolic influence on the differentiation of suppressive myeloid cells in cancer [J]. Carcinogenesis, 2018, 39(9): 1095-104.
39. YE H, ZHOU Q, ZHENG S, et al. Tumor-associated macrophages promote progression and the Warburg effect via CCL18/NF-kB/VCAM-1 pathway in pancreatic ductal adenocarcinoma [J]. Cell Death Dis, 2018, 9(5): 453.
40. YING H, KIMMELMAN A C, LYSSIOTIS C A, et al. Oncogenic Kras maintains pancreatic tumors through regulation of anabolic glucose metabolism [J]. Cell, 2012, 149(3): 656-70.

Figures

Figure 1

Workflow of our study.

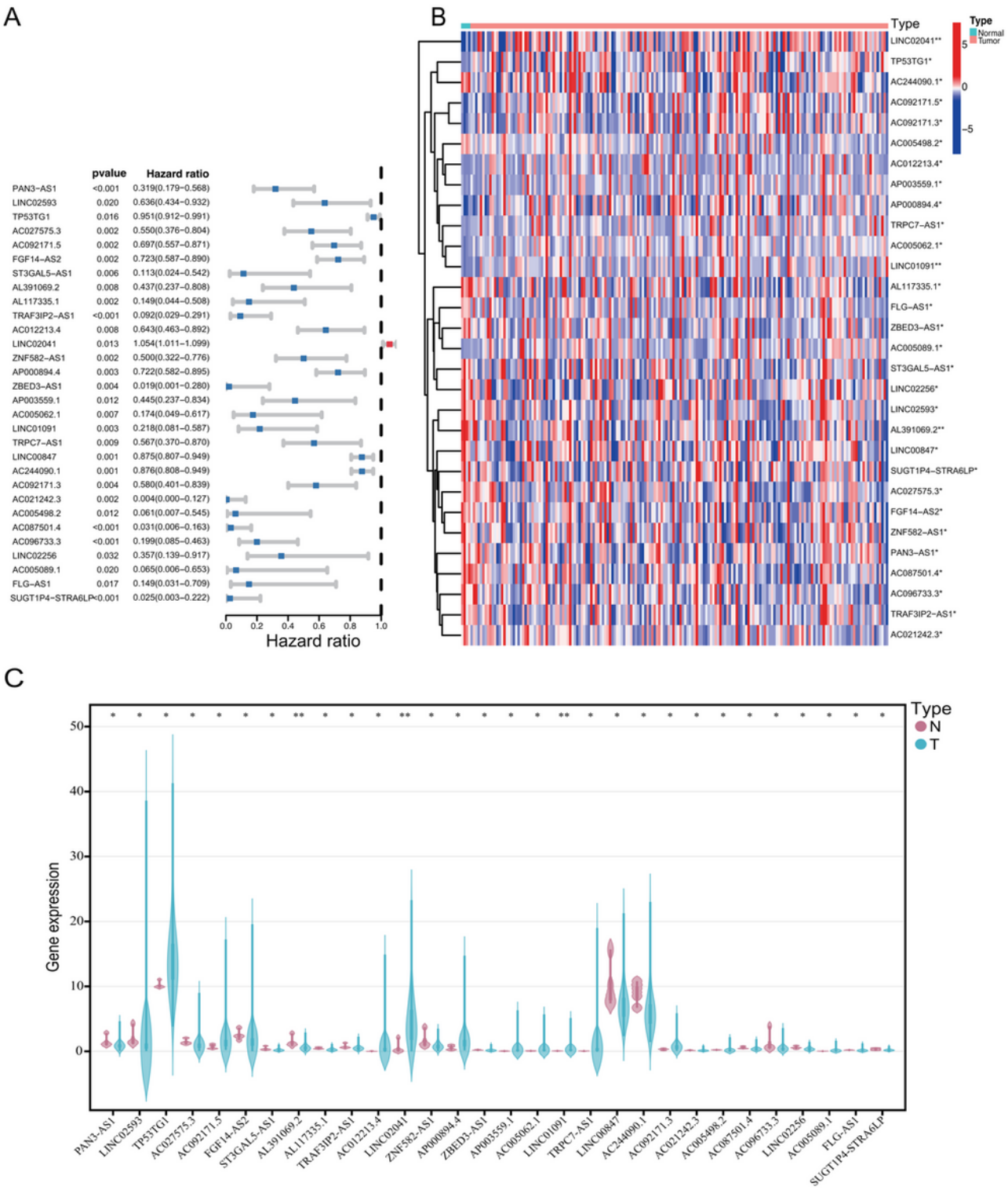

Figure 2

Prognostic cuproptosis-related lncRNAs. (A) Forest map of 30 prognostic cuproptosis-related lncRNAs identified by univariate Cox regression analysis. (B) Heatmap and (C) violin plot of the expression levels of prognostic CRLs in PC and adjacent normal pancreatic tissues. * $p < 0.05$ and ** $p < 0.01$.

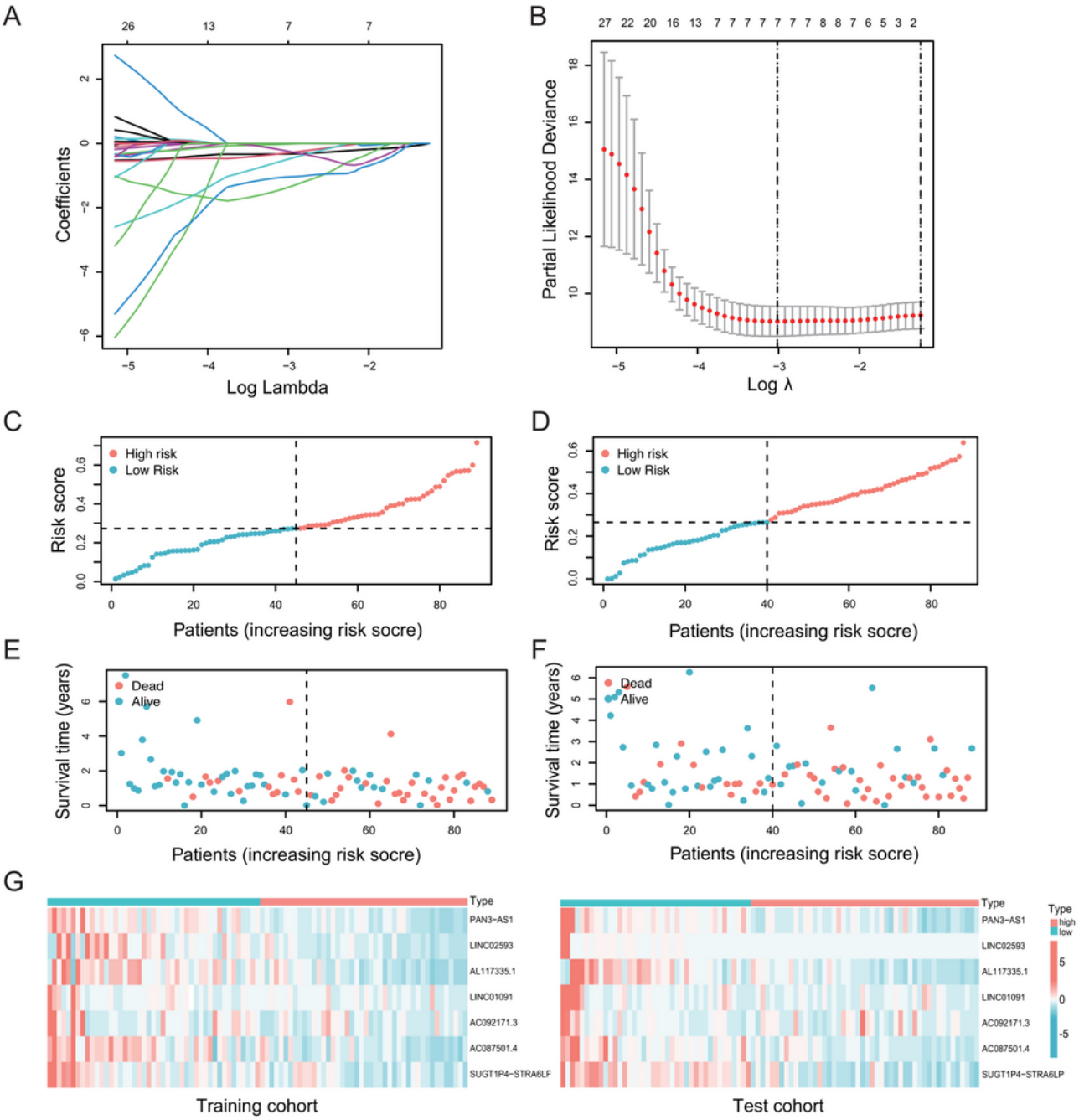

Figure 3

Construction of the prognostic model. (A, B) LASSO Cox regression and cross-validation of 30 prognostic CRLs. Distribution of risk scores of PC patients in (C) the training cohort and (D) the test cohort. Distribution of survival status of PC patients in (E) the training cohort and (F) the test cohort. (G) Heatmap of 7 risk signature genes in the training cohort and the test cohort.

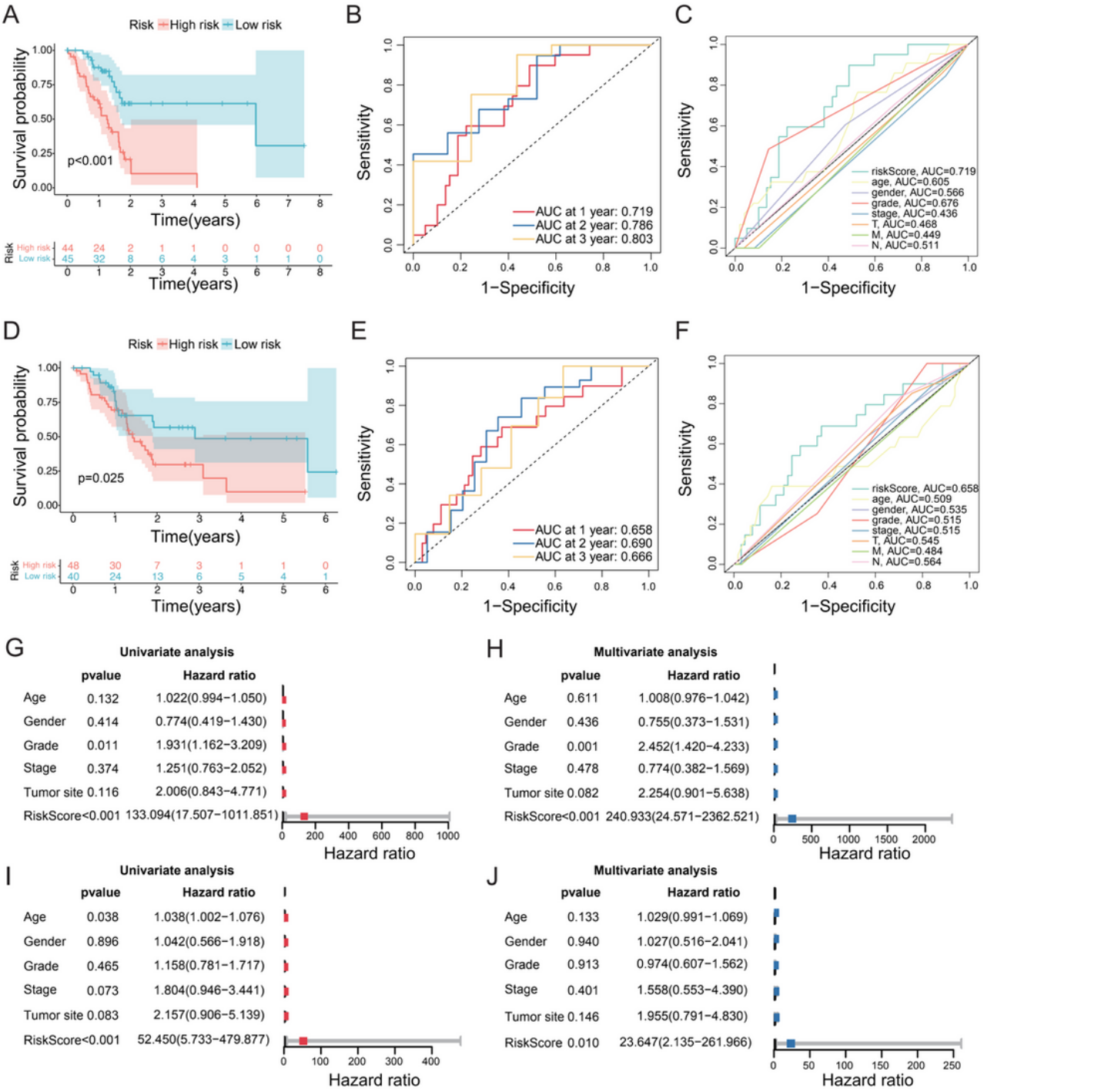

Figure 4

Prediction capacity analyses. (A) Kaplan–Meier survival curve of risk groups in the training cohort. (B) Time-dependent ROC curve of the risk model for 1, 2, and 3 years in the training cohort. (C) Time-dependent ROC curve of clinical characteristics in the training cohort. (D) Kaplan–Meier survival curve and (E, F) the ROC curve in the test cohort. Univariate and multivariate Cox regression analyses in (G, H) the training cohort and (I, J) the test cohort.

Figure 5

Independence analysis of prognostic signature. (A-F) Association of risk score and clinical characteristics. (G) Heatmap of seven prognostic CRLs expression levels and clinical characteristics (* $p < 0.05$). (H-O) Kaplan–Meier survival curves in different clinical subgroups.

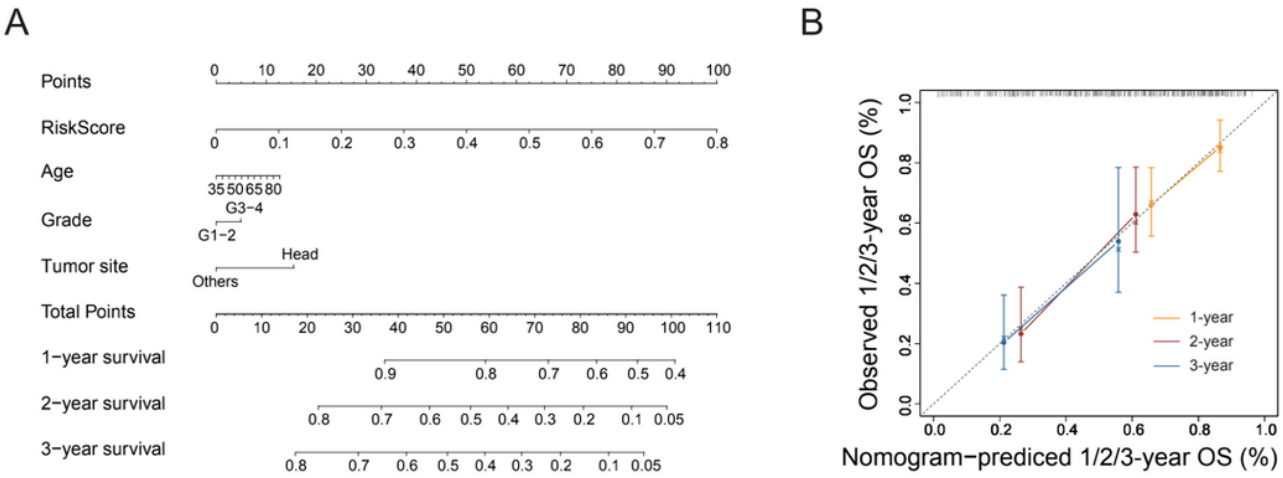

Figure 6

Construction and calibration of survival prediction nomogram in PC. (A) A nomogram for predicting the survival rates of 1-, 2-, and 3-year based on risk score and clinical features, including age, tumor tissue grade, and tumor site (head of the pancreas and others). (B) Calibration curve of the nomogram.

Figure 7

Immune analysis in CRLs risk model. (A-F) Correlation of immune cells and risk scores. (G) Immune cell infiltration in risk groups. (H) Tumor purity in high- and low-risk groups calculated by ESTIMATE algorithm (* $p < 0.05$ and ** $p < 0.01$). (I) Stroma score, immune score, and ESTIMATE score in risk groups.

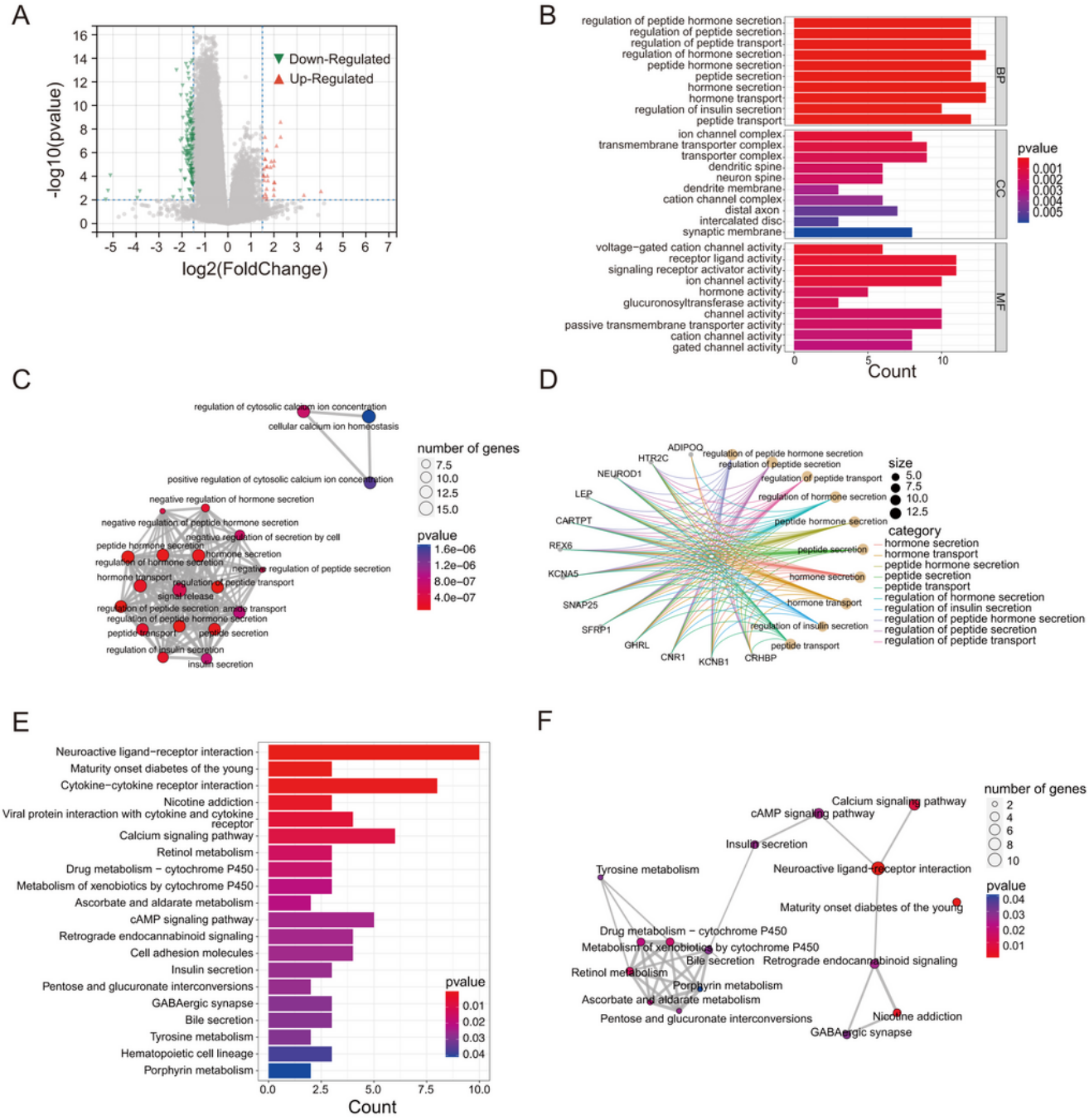

Figure 8

Functional enrichment analysis of DEGs. (A) The DEGs between the two risk groups were shown in a Volcano plot. (B) Bar plot shows the biological process (BP), cellular component (CC), and molecular function (MF) by GO analysis. (C) Network and (D) circle plot visualize the biological process by GO analysis. (E) Bar plot and (F) network shows the signaling pathways enriched by KEGG analysis.